Supporting Information

The Separator of Polyacrylonitrile Modified with Prussian Blue Analogs for High-efficiency Aqueous Zinc-ion Batteries

Junwei Chen, Zhiman Bai, Xinxin Yu, Wen Zhang, Tongtong Jiang and Mingzai Wu**

J. W. Chen, Dr. Z. M. Bai, Dr. X. X. Yu, Dr. W. Zhang, Dr. T. T. Jiang and Prof. M. Z. Wu
School of Materials Science and Engineering, Key Laboratory of Photoelectric Conversion Energy Materials and Devices of Anhui Province, Anhui university, Hefei 230601, China.
E-mail: wumz@ahu.edu.cn, baizhiman@ahu.edu.cn

Keywords: Prussian blue analogs, separators, zinc dendrites, zinc ion batteries

Experimental section

Materials:

Nickel nitrate hexahydrate ($Ni(NO_3)_2 \cdot 6H_2O$, AR), potassium ferricyanide ($K_3Fe(CN)_6$), N,N-dimethylformamide (DMF), polyacrylonitrile (PAN, average molecular weight of 149,000 ~ 151,000), carboxyl-multiwalled carbon nanotubes (CNT, diameter of 10 ~ 30 nm and length of 5 ~ 30 μm), potassium permanganate ($KMnO_4$, AR), manganese acetate tetrahydrate ($Mn(CH_3COO)_2 \cdot 4H_2O$, AR), N-methyl-2-pyrrolidone (NMP, AR) were purchased from Shanghai Aladdin Biochemical Technology Co., Ltd. Sodium citrate dihydrate ($C_6H_5Na_3O_7 \cdot 2H_2O$,), acetylene blacks and Poly(vinylidene fluoride) (PVDF) binder were purchased from Shanghai Macklin biochemical Co., Ltd. Zinc foil and titanium foil were purchased from Hefei Wenghe Metal Materials Co., Ltd.

Synthesis of FeNi-PBA nanoparticles:

Firstly, 0.58 g $Ni(NO_3)_2 \cdot 6H_2O$ and 0.66 g $C_6H_5Na_3O_7 \cdot 2H_2O$ were dissolved in 50 mL deionized water with stirring until the formation of homogeneous solution, followed by the addition of the mixture solution of 0.43 g $K_3Fe(CN)_6$ and 50 mL deionized water. After being stirred for 10 min and aged at room temperature for 24 h, the precipitate turned up in the mixed solution, which was then collected by centrifugation, washed for three times with deionized water and ethanol, respectively, and finally dried at 100 ^oC for 24 h in vacuum oven. The obtained light blue product was FeNi-based prussian blue analogue nanoparticles and labelled as FeNi-PBA.

Fabrication of FeNi-PBA@PAN and PAN separators:

1.0 g FeNi-PBA powder and 2.0 g PAN were dispersed in 18.0 g DMF with stirring for 12 h. Then, the obtained solution with high viscosity was put into a syringe for electrospinning with roller rotation speed of 400 r/min, high voltage of 11.5 kV, receiving distance of 10 cm, flow rate of 0.6 mL h^{-1}. After electrospinning for 80 min, the obtained nanofiber separator was dried in a vacuum oven at 120 °C for 24 h, forming the light-yellow product (labelled as FeNi-PBA@PAN). Comparatively, PAN nanofiber separator was also fabricated with similar preparation processing to that of FeNi-PBA@PAN without FeNi-PBA powder.

Preparation of MnO_2 Cathode:

MnO_2/CNT composite was synthesized according to our previous work [1]. 0.2 g CNT was dispersed in 120 mL deionized water, then 0.973 g $KMnO_4$ was added into the above solution with continuous stirring for 0.5 h. Subsequently, $Mn(CH_3COO)_2 \cdot 4H_2O$ solution (2.27 g dissolved in 20 mL deionized water) was added dropwise into the above solution with stirring for 1 h. Thereafter, the solution was transferred into a Teflon-lined autoclave and heated at 120 °C for 12 h. After cooling, the obtained dark brown precipitate was filtered and washed with

deionized water. Finally, the MnO_2/CNT composite was obtained after being dried overnight in a vacuum oven at room temperature. To prepare the cathode, MnO_2/CNT composite, acetylene blacks and PVDF binder were mixed with a mass ratio of 7.5:1.5:1 using NMP as solvent. The mixtures were then stirred for 3 h and coated with a blade on a piece of carbon cloth, followed by being dried in a vacuum oven at 40 °C. The effective mass loading of MnO_2 is about 3.0 mg cm^{-2}.

Cell assembling:

Zn||Zn symmetrical battery and Zn||Ti half-cell were assembled based on the case of CR2032 model coin cell using 2M $ZnSO_4$ as the electrolyte, and a Zn||MnO_2/CNT battery was assembled using 2M $ZnSO_4$ and 0.1M $MnSO_4$ as the electrolyte.

Soft pack battery assembling:

Pure zinc foil with size of 50 mm × 40 mm was used as the andoe of the battery. Carbon cloth coated with MnO_2/CNT with the same size was used as the cathode of the battery. FeNi-PBA@PAN with size of 52 mm × 42 mm was used as the battery separator. Firstyly, 200 μL of electrolyte (2 M $ZnSO_4$ + 0.1 M $MnSO_4$) was dropped on the surface of the FeNi-PBA@PAN separator, which was then stacked on the zinc foil. Then, the carbon cloth coated with MnO_2/CNT was stacked on the surface of the separator, forming a sandwich structure, which was further wrapped with aluminum-plastic film, and sealed by extracted vacuum.

Material characterizations:

The characterization instruments used in this study were field emission scanning electron microscopy (FE-SEM, S-4800, Hitachi), X-ray powder diffractometer (XRD Bruker D8-ADVANCE), X-ray photoelectron spectroscopy (XPS, Escalab 250Xi) and transmission electron microscopy (TEM JEM-2100, JEOL). White light interference profiler (Bruker Contour GT-K 3D) was used to observe the microscopic morphology of the sample surface, and a Malvern nano laser particle sizer (Zetasizer Nano ZS90) was used to detect the ZETA potential.

Electrochemical measurements:

Electrochemical tests were carried out on the assembled Zn||Zn symmetrical batteries, Zn||Ti half batteries and Zn||MnO_2/CNT full batteries using electrochemical workstation (CHI760E, Shanghai). The battery test system (LAND-CT2001A, Wuhan) was used to test the cyclic stability of Zn||Zn symmetrical batteries and Zn||MnO_2/CNT full batteries. The Zn^+ transference numbers t_{Zn}^{2+} of separators were tested by using AC impedance and DC potentiostatic polarization measurements with a Zn||Zn symmetric cell. The cell

was measured by a small DC polarization potential (10 mV) for enough time to reach a steady-state current. [2] The electrochemical impedance spectroscopy (EIS) measurements with the frequency range of 1 MHz to 0.01 Hz were performed on an electrochemical workstation (CHI760E, Shanghai). The t_{Zn}^{2+} was calculated according to the following equation:

$$t_{Zn^+} = \frac{I_S(\Delta - I_0 R_0)}{I_0(\Delta - I_S R_S)}$$

Where Δv is the potential applied across the cell. I_0 and I_S are the initial state current and steady state current, respectively. R_0 and R_S are the initial state resistance and steady state resistance, respectively.

Density functional theory calculations:

All the DFT calculations were conducted based on the Vienna Ab-inito Simulation Package (VASP). The theoretical models for the adsorption of SO_4^{2-} by PAN and FeNi-PBA in DFT simulations are shown in Fig. S3. The exchange-correlation effects were described by the Perdew-Burke-Ernzerhof (PBE) functional within the generalized gradient approximation (GGA) method. The core-valence interactions were accounted by the projected augmented wave (PAW) method. The energy cutoff for plane wave expansions was set to 480 eV, and the 3×3×1 Monkhorst-Pack grid k-points were selected to sample the Brillouin zone integration. The vacuum space is adopted 15 Å above the surfaces to avoid periodic interactions. The structural optimization was completed for energy and force convergence set at 1.0×10^{-4} eV and 0.02 eV $Å^{-1}$, respectively. The adsorption energy can be calculated according to the following formula:

$$E_{ads} = E(A+B) - E(A) - E(B)$$

where E_{ads} represents the adsorption energy, E(A+B) is the calculated energy of adsorption configuration, E(A) and E(B) mean the calculated energy of substrate and adsorbent respectively. The adsorption energy of FeNi-PBA for SO_4^{2-} anions is recorded as -1.78 eV, surpassing that of PAN for SO_4^{2-} anions, which stand at -1.47eV.

Multi-physical model development of PAN and GF separator near zinc anode surfaces.

The electrochemical simulation was carried out using the secondary current distribution physical field interface in the electrochemical module of COMSOL Multiphsics software. The area, size and boundary conditions are constructed by this model and shown in Fig. S7. The electrolyte current was solved according to Ohm's law. One of the electrodes was grounded and the other was set to the battery potential to satisfy the total current condition. The governing

equation is as follows:

$$i = -F\sum -z_i^2 m_i F c_i \nabla \Phi_i$$

i represents the current density vector (SI unit: A/m^2); z_i is the number of ionic charges; m_i stands for mobility (SI unit: mol×m^2×s×V×A), F stands for Faraday constant (SI unit: A×s/mol), Φ_i stands for ion potential, c_i stands for ion concentration. At the same time, the conservation of current density is satisfied:

$$\nabla \cdot i = 0$$

In the simulation, expressions in the form of Butler-Volmer are used to describe the electrode dynamics occurring on the electrode surface embedded in the electrolyte. Electrode surface current density refer to the Butler-Volmer equation:

$$i_a = i_0\left(\frac{c}{c_0}\exp\left(\frac{\eta(1-\beta)F}{(RT)}\right) - \exp\left(\frac{\eta\beta F}{(RT)}\right)\right)$$

The initial value of the electrolyte potential is set to be equivalent to the battery potential at open circuit (when the potential is not activated). The following is the definition of overpotential:

$$\eta = \Phi_s - \Phi_i - E_{\text{eq}}$$

Where η is the overpotential, Φ_s is the electrode potential, Φ_i is the electrolyte potential, and E_{eq} is the equilibrium potential. In terms of material setting, the conductivity of electrolyte was set to 4.5 S/m and the conductivity of electrode material was set to 1e^7 S/m; in terms of boundary setting, the bottom of the electrode was set as the reference 0 V potential, and the top was set as the average current density boundary of 5 mA cm^{-2}.

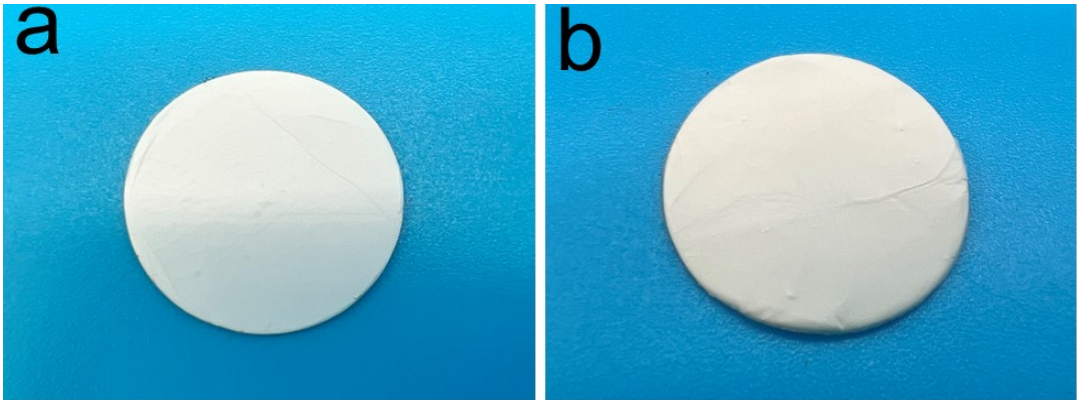

Fig. S1 Optical images of a) PAN separator and b) FeNi-PBA@PAN separator.

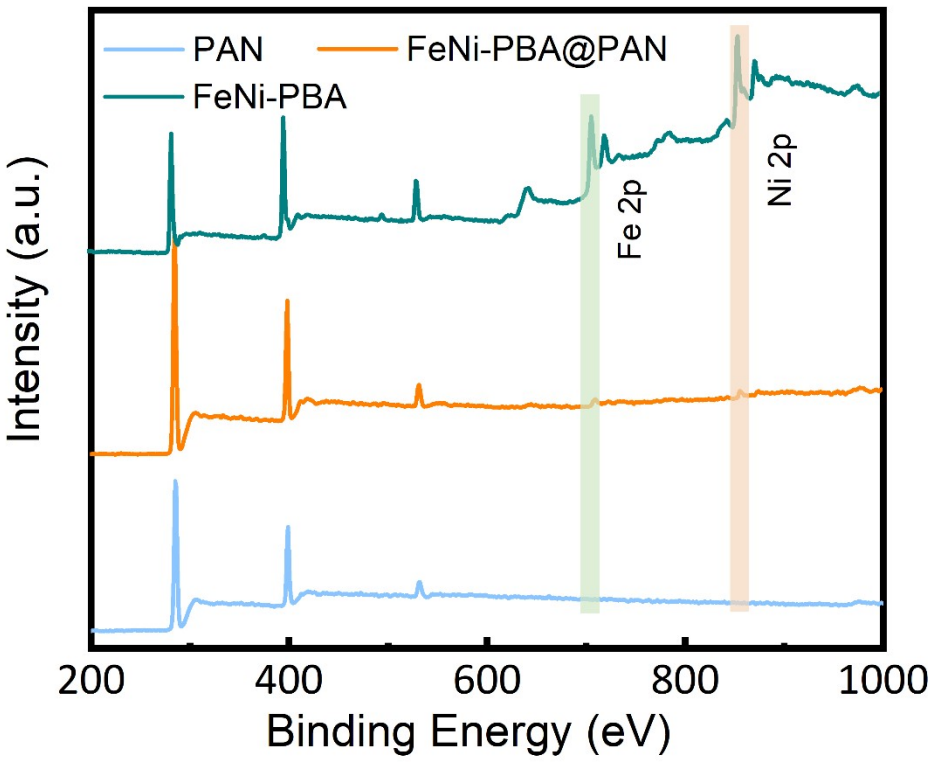

Fig. S2 Full XPS spectra of FeNi-PBA@PAN, FeNi-PBA, and PAN.

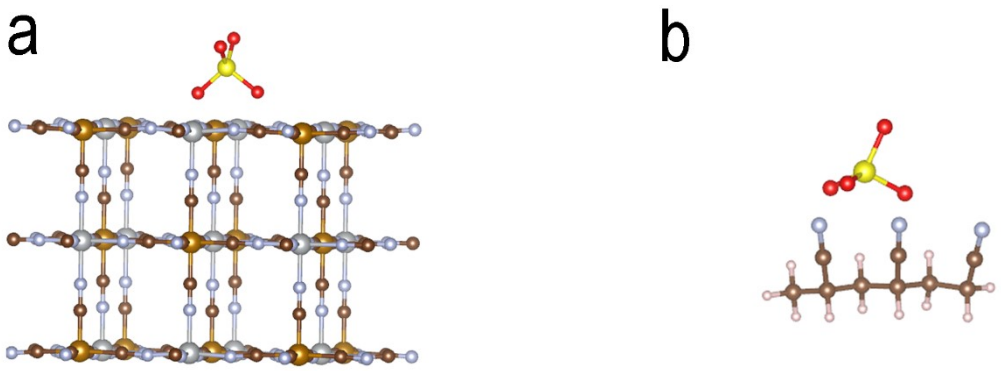

Fig. S3 Model structure of FeNi-PBA and PAN.

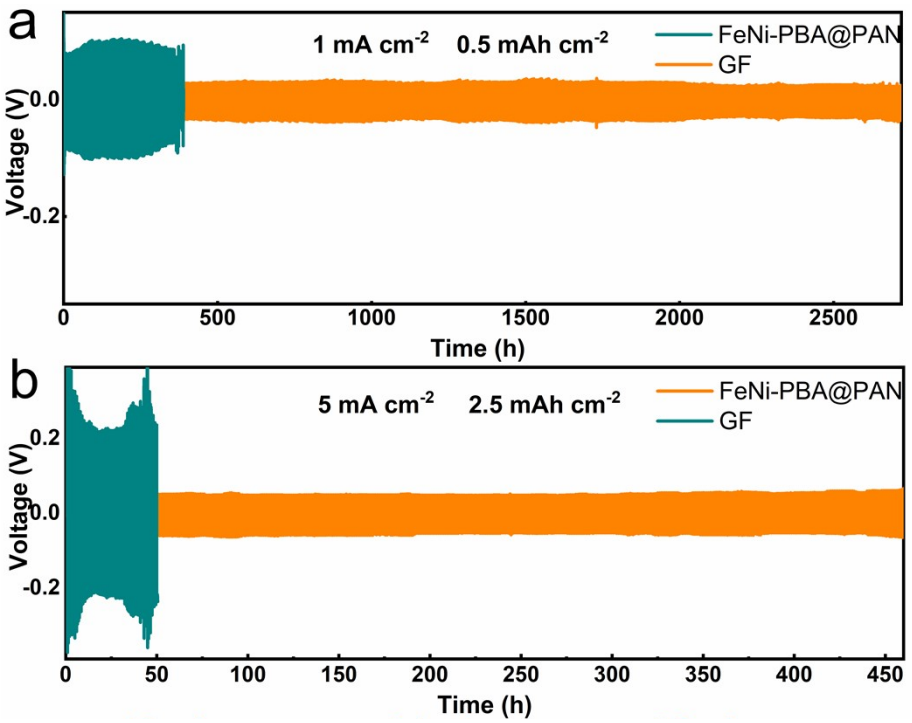

Fig. S4 Long-term galvanostatic charge/discharge cycling voltage profiles of Zn||Zn symmetric cells using GF and FeNi-PBA@PAN separators at a current density of a) 1.0 mA cm^{-2} with the cutoff capacity of 0.5 mAh cm^{-2} and b) 5.0 mA cm^{-2} with the cutoff capacity of 2.5 mAh cm^{-2}.

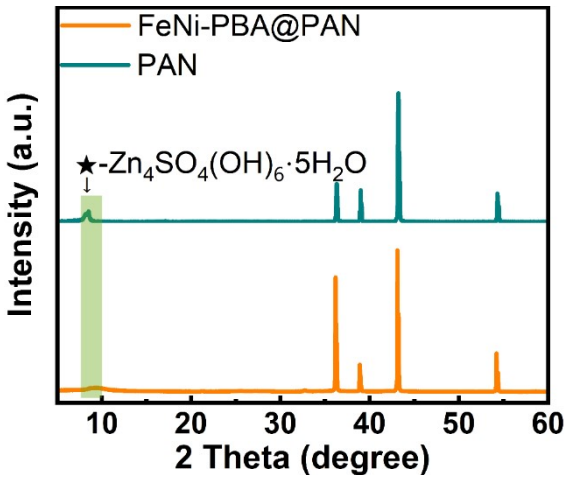

Fig. S5 XRD patterns of Zn anode surface in Zn||Zn symmetric batteries using PAN and FeNi-PBA@PAN separators after 100 h galvanostatic charge/discharge cycling test at a current density of 5.0 mA cm^{-2} with the cutoff capacity of 2.5 mAh cm^{-2}.

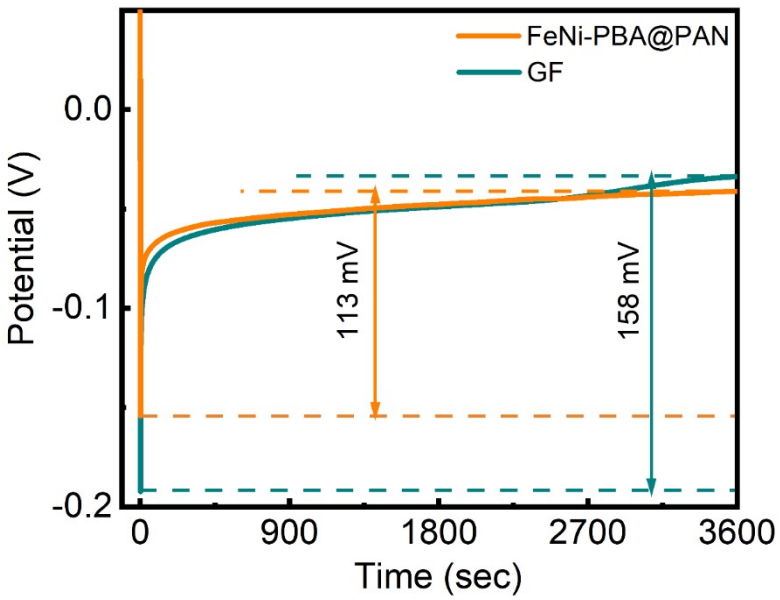

Fig. S6 Nucleation overpotentials of Zn|FeNi-PBA@PAN|Ti and Zn|GF|Ti.

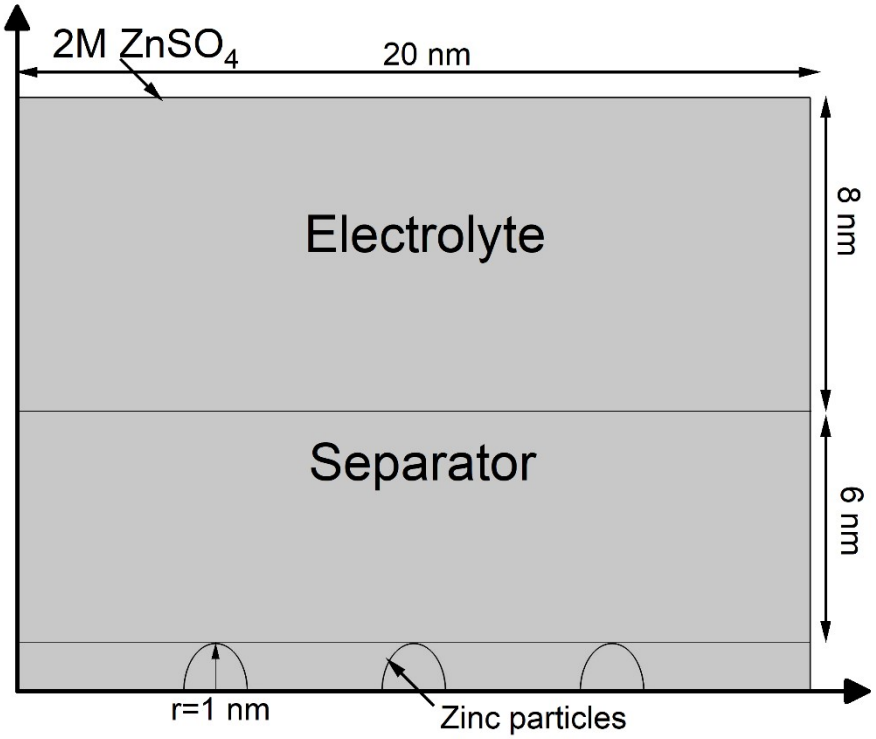

Fig. S7 Simulated domains and dimensions used in this study.

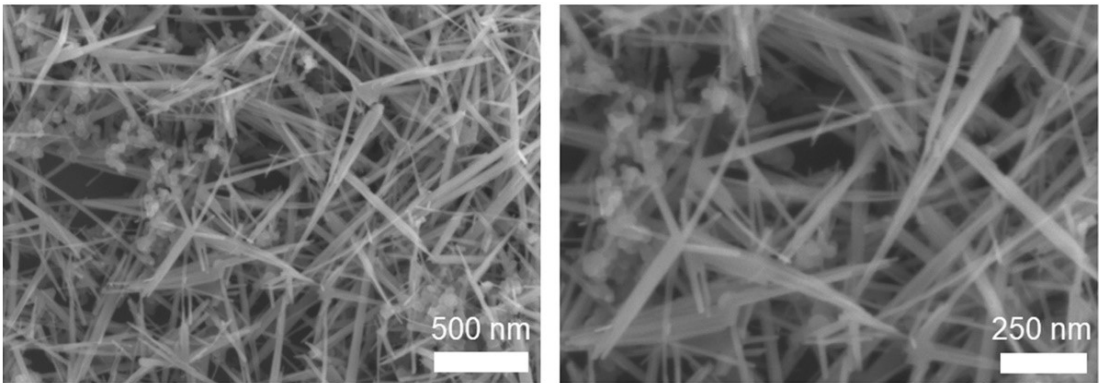

Fig. S8 SEM images of MnO_2/CNT.

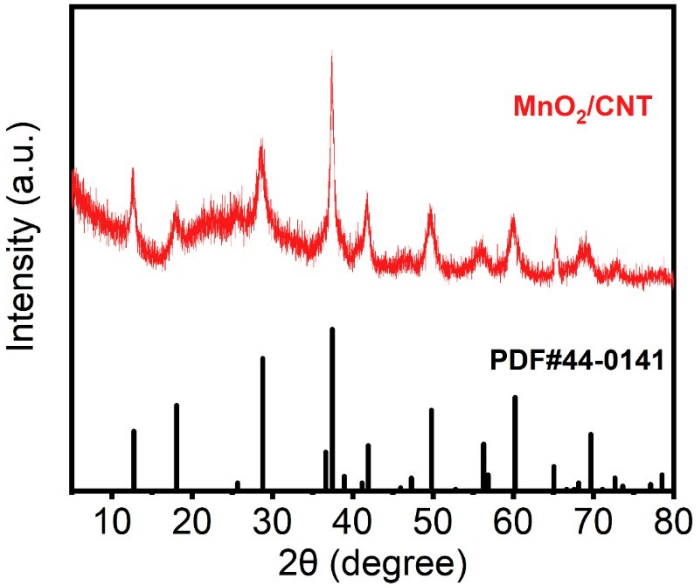

Fig. S9 XRD pattern of MnO_2/CNT.

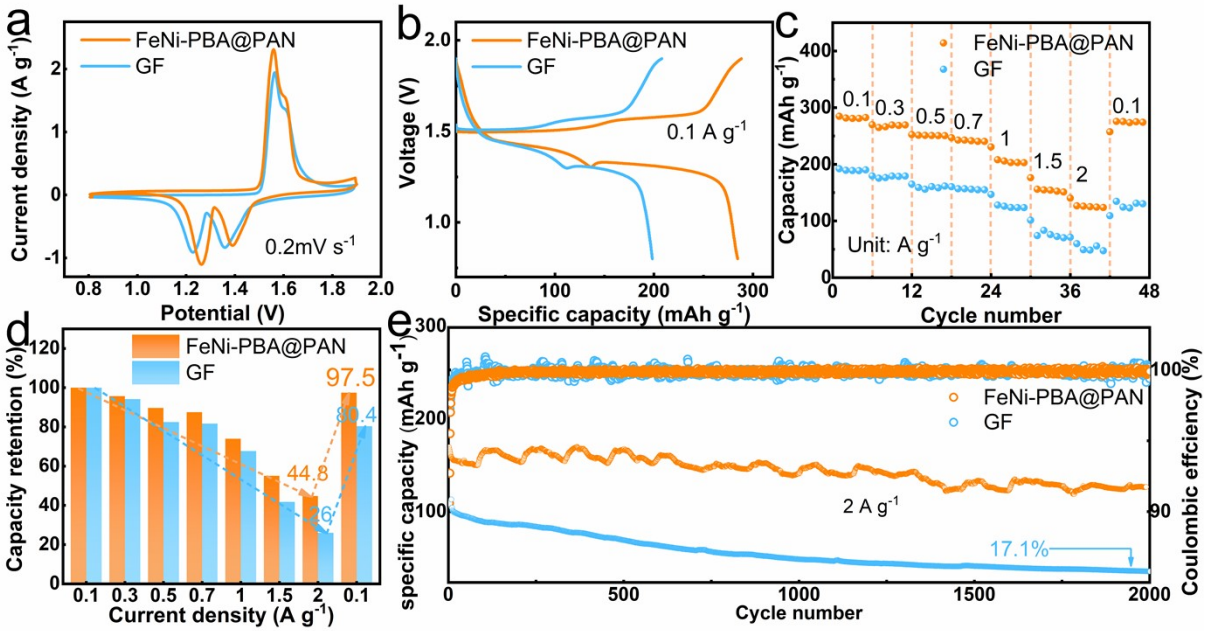

Fig. S10 Electrochemical performance of Zn||MnO_2/CNT full batteries using GF and FeNi-PBA@PAN separators. a) CV curves at 0.2 mV s^{-1}. b) Charge-discharge curves at a current density of 0.1 A g^{-1}. c) Rate performance and d) the corresponding capacity retention. e) Long-term cycling performance at a current density of 2 A g^{-1}.

Table S1. Summarized table of the cycle life of Zn||Zn symmetrical cells using the modified separators and Zn anodes.

Strategies	Materials	Current density (mA cm^{-2})	Areal capacity (mAh cm^{-2})	Cycle life (h)	Ref.
Separator modification	FeNi-PBA @PAN	1	0.5	2750	This work
	PAN		0.283	800	[3]
	MOF808@GFC	0.1		350	[4]
	g-C3N4 coated separator	1	0.25	770	[5]
	UiO-66-COOH/rGO interlayers	2	1	500	[6]
	GF/PANI	0.5	0.5	2700	[7]
	ZnHAP/BC	1	1	1600	[8]
Artificial interface modification	UiO-66@Zn	1	0.5	250	[9]
	ZnSe@Zn	1	0.5	1700	[10]
	CeO2@Zn	0.5	0.25	1300	[11]
	Zn@SA @TiO2-MS	0.5	0.25	2650	[12]
	GaIn@Zn	1	0.1	1200	[13]
	rGO@Zn	1	1	300	[14]
	ZnF2@Zn	0.5	0.5	700	[15]
	SCM@Zn	2	1	500	[16]
	In@Zn	4	1	400	[17]
	PPy@Zn	2	1	540	[18]
	TZNC@Zn	1	1	450	[19]
	Zn@IS	0.5	0.5	3000	[20]

References

[1] D. H. Wang, H. F. Li, Z. X. Liu, Z. J. Tang, G. J. Liang, F. N. Mo, Q. Yang, L. T. Ma, C. Y. Zhi, *Small.* **2018**, *14*, 1803978.

[2] J. Evans, C. A. Vincent, P. G. Bruce, *Polymer.* **1987***, 28,* 2324-2328.

[3] Y. Fang, X. Xie, B. Zhang, Y. Chai, B. Lu, M. Liu, J. Zhou, S. Liang, *Adv. Funct. Mater.* **2021**, *32,* 2109671.

[4] N. Maeboonruan, J. Lohitkarn, C. Poochai, T. Lomas, A. Wisitsoraat, S. Kheawhom, S. Siwamogsatham, A. Tuantranont, C. Sriprachuabwong, *J. Sci.: Adv. Mater. Devices.* **2022**, *7,* 100467.

[5] L. Wu, Y. Zhang, P. Shang, Y. Dong, Z.-S. Wu, *J. Mater. Chem. A.* **2021**, *9*, 27408-27414.

[6] Z. Wang, L. Dong, W. Huang, H. Jia, Q. Zhao, Y. Wang, B. Fei, F. Pan, *Nano-Micro Lett.* **2021**, *13*, 73.

[7] F. Wu, F. Du, P. Ruan, G. Cai, Y. Chen, X. Yin, L. Ma, R. Yin, W. Shi, W. Liu, J. Zhou, X. Cao, *J. Mater. Chem. A.* **2023**, *11*, 11254-11263.

[8] H. Qin, W. Chen, W. Kuang, N. Hu, X. Zhang, H. Weng, H. Tang, D. Huang, J. Xu, H. He, *Small.* **2023**, *19*, e2300130.

[9] M. Liu, L. Yang, H. Liu, A. Amine, Q. Zhao, Y. Song, J. Yang, K. Wang, F. Pan, *ACS. Appl. Mater. Interf.* **2019**, *11*, 32046-32051.

[10] T. C. Li, Y. V. Lim, X. Xie, X. L. Li, G. Li, D. Fang, Y. Li, Y. S. Ang, L. K. Ang, H. Y. Yang, *Small.* **2021**, *17*, e2101728.

[11] H. Liu, J. G. Wang, W. Hua, H. Sun, Y. Huyan, S. Tian, Z. Hou, J. Yang, C. Wei, F. Kang, *Adv. Sci.* **2021**, *8*, e2102612.

[12] H. Zhang, Y. Wu, J. Yu, T. Jiang, M. Wu, *Adv. Funct. Mater.* **2024**, *34*, 2301912.

[13] C. Liu, Z. Luo, W. Deng, W. Wei, L. Chen, A. Pan, J. Ma, C. Wang, L. Zhu, L. Xie, X.-Y. Cao, J. Hu, G. Zou, H. Hou, X. Ji, *ACS. Energy. Lett.* **2021**, *6*, 675-683.

[14] A. Xia, X. Pu, Y. Tao, H. Liu, Y. Wang, *Appl. Surf. Sci.* **2019**, *481*, 852-859.

[15] J. Han, H. Euchner, M. Kuenzel, S. M. Hosseini, A. Groß, A. Varzi, S. Passerini, *ACS. Energy. Lett.* **2021**, *6*, 3063-3071.

[16] Y. Zou, X. Yang, Z. Xue, Y. Su, C. Qiao, W. Guo, Z. Chen, J. Sun, *J. Phys. Chem. C.* **2022**, *126*, 21205-21212.

[17] K. Hu, X. Guan, R. Lv, G. Li, Z. Hu, L. Ren, A. Wang, X. Liu, J. Luo, *Chem. Eng. J.* **2020**, *396*.

[18] F. Zhang, C. Wang, J. Pan, F. Tian, S. Zeng, J. Yang, Y. Qian, *Mater. Today Energy.* **2020**, *17,* 100443.

[19] P. X. Sun, Z. Cao, Y. X. Zeng, W. W. Xie, N. W. Li, D. Luan, S. Yang, L. Yu, X. W. D. Lou, *Angew. Chem. Int. Ed.* **2022**, *61*, e202115649.

[20] S. Jiao, J. Fu, M. Wu, T. Hua, H. Hu, *ACS Nano* **2022**, *16*, 1013-1024.